Research Article | Vol. 7, No. 2 | 1 Feb 2017 | OPTICAL MATERIALS EXPRESS 494

Optical Materials EXPRESS

Effective control over near band-edge emission in ZnO/CuO multilayered films

Bunyod Allabergenov,[1,2] Ulugbek Shaislamov,[3] Hyunseok Shim,[1] Myeong-Jae Lee,[1] Anvar Matnazarov,[2] and Byeongdae Choi[1,*]

[1]*Nano and Bio Research Division, Daegu Gyeongbuk Institute of Science and Technology (DGIST), 50-1 Sang-Ri, Heyonpung-Myeon, Dalseong-Gun, Daegu 711-873, South Korea*
[2]*Department of Transport Systems, Urgench State University (USU), 14 Khamid Alimjon, Urgench 220-100, Uzbekistan*
[3]*Department of the advanced Materials and Engineering, Jeju National University, 1 Arail-dong, Jeju-si, Jeju-do, South Korea*
**bdchoi1@dgist.ac.kr*

Abstract: We report on a study of the microstructural and photoluminescent properties of ZnO/CuO multilayered films. Multilayered ZnO/CuO thin films were deposited on amorphous SiO_2/Si substrates by a pulsed laser technique and their microstructural and optical properties were characterized by transmission electron microscopy (TEM) and photoluminescence spectroscopy. TEM and XRD analyses of annealed ZnO/CuO films reveal the formation of multiple crystallographic defects and modification of the dominant growth plane, indicating effective doping of Cu atoms into the ZnO lattice. Consequently, near-band-edge emission in ZnO can be controlled through the number of CuO layers. Redshift of the near-band-edge emission peak from 385 nm up to 422 nm is achieved by increasing the number of CuO layers up to a certain number, above which a downward shift is observed. The results demonstrate that the emission properties of ZnO can be modified and precisely controlled by incorporation of CuO thin layers as a Cu-doping source.

© 2017 Optical Society of America

OCIS codes: (310.0310) Thin films; (310.6860) Thin films, optical properties; (250.5230) Photoluminescence; (160.4670) Optical materials.

References and links

1. Ü. Özgür, Ya. I. Alivov, C. Liu, A. Teke, M. A. Reshchikov, S. Doğan, V. Avrutin, S.-J. Cho, and H. Morkoç, "A comprehensive review of ZnO materials and devices," J. Appl. Phys. **98**(4), 041301 (2005).
2. M. D. McCluskey and S. J. Jokela, "Defects in ZnO," J. Appl. Phys. **106**(7), 071101 (2009).
3. A. O. Dikovska, P. A. Atanasov, T. R. Stoyanchov, A. T. Andreev, E. I. Karakoleva, and B. S. Zafirova, "Pulsed laser deposited ZnO film on side-polished fiber as a gas sensing element," Appl. Opt. **46**(13), 2481–2485 (2007).
4. U. Shaislamov, K. Krishnamoorthy, S. J. Kim, A. Abidov, B. Allabergenov, S. Kim, S. Choi, R. Suresh, W. M. Ahmed, and H.-J. Lee, "Highly stable hierarchial p-CuO/ZnO nanorod/nanobranch photoelectrode for efficient solar energy conversion," Int. J. Hydrogen Energy **41**(4), 2253–2262 (2016).
5. Y.-S. Choi, J.-W. Kang, D.-K. Hwang, and S.-J. Park, "Recent advances in ZnO-based light-emitting diodes," IEEE Trans. Electron Dev. **57**(1), 26–41 (2010).
6. F. M. Li, L. T. Bo, S. Y. Ma, X. L. Huang, L. G. Ma, J. Liu, X. L. Zhang, F. C. Yang, and Q. Zhao, "Effects of the oxygen partial pressure and annealing atmospheres on the microstructures and optical properties of Cu-doped ZnO films," Superlattices Microstruct. **51**(3), 332–342 (2012).
7. R. Hussin, K.-L. Choy, and X. Hou, "Fabrication of multilayer ZnO/TiO_2/ZnO thin films with enhancement of optical properties by atomic layer deposition (ALD)," http://www.scientific.net/AMM.465-466.916.
8. B. Choi, H. Shim, and B. Allabergenov, "Red photoluminescence and blue-shift caused by phase transformation in multilayer films of titanium dioxide and zinc sulfide," Opt. Mater. Express **5**(10), 2156 (2015).
9. B. Allabergenov, S.-H. Chung, S. Kim, and B. Choi, "Optical properties of Cu-doped ZnO thin films prepared by Cu solution coating," J. Nanosci. Nanotechnol. **15**(10), 7664–7670 (2015).
10. J.-H. Kim, T.-H. Shin, K.-J. Yang, J. Jeong, and B. Choi, "Abstraction of blue photoluminescence in Al-doped ZnO nanoparticles prepared by electron beam deposition," Appl. Phys. Express **5**(1), 012603 (2012).
11. M. Wang, E. W. Shin, J. S. Chung, S. H. Hur, E. J. Kim, S. H. Hahn, and K.-K. Koo, "Tunable visible emission and warm white photoluminescence of lithium-doped zinc oxide thin films," J. Mater. Sci. **45**(15), 4111–4114 (2010).
12. S. Chirakkara and S. B. Krupanidhi, "Pulsed laser deposited ZnO/ZnO:Li multilayer for blue light emitting diodes," J. Lumin. **131**(8), 1649–1654 (2011).

#282564 http://dx.doi.org/10.1364/OME.7.000494
Journal © 2017 Received 8 Dec 2016; revised 30 Dec 2016; accepted 30 Dec 2016; published 19 Jan 2017

Optical Materials EXPRESS

13. B. Allabergenov, S.-H. Chung, S. M. Jeong, S. Kim, and B. Choi, "Enhanced blue photoluminescence realized by copper diffusion doping of ZnO thin films," Opt. Mater. Express **3**(10), 1733 (2013).
14. S. Fujihara, Y. Ogawa, and A. Kasai, "Tunable visible photoluminescence from ZnO thin films through Mg-doping and annealing," Chem. Mater. **16**(15), 2965–2968 (2004).
15. P. Bhattacharya, R. R. Das, and R. S. Katiyar, "Fabrication of stable wide-band-gap ZnO/MgO multilayer thin films," Appl. Phys. Lett. **83**(10), 2010–2012 (2003).
16. A. Kaushal and D. Kaur, "Pulsed laser deposition of transparent ZnO/MgO multilayers," J. Alloys Compd. **509**(2), 200–205 (2011).
17. J. M. Jensen, A. B. Oelkers, R. Toivola, D. C. Johnson, J. W. Elam, and S. M. George, "X-ray reflectivity characterization of ZnO/Al_2O_3 multilayers prepared by atomic layer deposition," Chem. Mater. **14**(5), 2276–2282 (2002).
18. K. C. Sekhar, K. Kamakshi, S. Bernstrorff, and M. J. M. Gomes, "Effect of annealing temperature on photoluminescence and resistive switching characteristics of ZnO/Al_2O_3 multilayer nanostructures," J. Alloys Compd. **619**, 248–252 (2015).
19. W. S. Choi, E. J. Kim, S. G. Seong, Y. S. Kim, C. Park, and S. Hahn, "Optical and structural properties of ZnO/TiO_2/ZnO multi-layers prepared via electron beam evaporation," Vacuum **83**(5), 878–882 (2009).
20. Y. J. Park, J. H. Yang, B. D. Ryu, J. Cho, T. V. Cuong, and C.-H. Hong, "Solution-processed multidimensional ZnO/CuO heterojunction as ultraviolet sensing," Opt. Mater. Express **5**(8), 1752 (2015).
21. H. Kidowaki, T. Oku, and T. Akiyama, "Fabrication and evaluation of CuO/ZnO heterostructures for photoelectric conversion," I.J.R.RAS **13**(1), 67–72 (2012).
22. Y. Yan, M. M. Al-Jassim, and S. H. Wei, "Doping of ZnO by group-IB elements," Appl. Phys. Lett. **89**(18), 181912 (2006).
23. X. Peng, J. Xu, H. Zang, B. Wang, and Z. Wang, "Structural and PL properties of Cu-doped ZnO films," J. Lumin. **128**(3), 297–300 (2008).
24. L. Ma, S. Ma, H. Chen, X. Ai, and X. Huang, "Microstructures and optical properties of Cu-doped ZnO films prepared by radio frequency reactive magnetron sputtering," Appl. Surf. Sci. **257**(23), 10036–10041 (2011).
25. B. Allabergenov, O. Tursunkulov, A. I. Abidov, B. Choi, J. W. Jeong, and S. Kim, "Microstructural analysis and optical characteristics of Cu-doped ZnO thin films prepared by DC magnetron sputtering," in *Proceedings of 17th International Conference on Crystal Growth and Epitaxy*, P. Gille, W. Miller, K. Sangwal and E. Talik, ed. (Elsevier, 2014), pp. 573–576.
26. B. Allabergenov, O. Tursunkulov, S. J. Jo, A. Abidov, C. Gomez, S. B. Park, and S. Kim, "Fabrication of copper-graphite composites by spark plasma sintering and its characterization," in a *book chapter of Advances in Sintering Science and Technology II: Ceramic Transactions*, S. -J. L. Kang, R. Bordia, E. Olevsky and D. Bouvard, eds. (The American Ceramic Society, 2012), pp. 151–161.
27. Y. Wang, X. Li, G. Jiang, W. Liu, and C. Zhu, "Origin of (103) plane of ZnO films deposited by RF magnetron sputtering," J. Mater. Sci. Mater. Electron. **24**(10), 3764–3767 (2013).
28. D. Das and P. Mondal, "Photoluminescence phenomena prevailing in c-axis oriented intrinsic ZnO thin films prepared by RF magnetron sputtering," RSC Advances **4**(67), 35735 (2014).
29. R. Oommen, U. Rajalakshmi, and C. Sanjeeviraja, "Characteristics of electron beam evaporated and electrodeposited Cu2O thin films-comparative study,", Int. J. Electrochem. Sci. **7**(9), 8288–8298 (2012).

1. Introduction

Zinc oxide (ZnO) has attracted much attention as a candidate material for the next generation of solid state lighting devices because of its wide bandgap and high excitonic binding energy, in addition to an emission wavelength tunable from the UV to the visible light region. Further, ZnO has been recognized as an important platform for various applications such as optoelectronic devices, thin film gas sensors, solar energy converters, antireflection coatings, light emitting diodes (LEDs), and laser diodes [1–5]. Recent reports on ZnO thin films have shown the possibility of controlling its photoluminescence (PL) properties in the UV and visible light range by heat treatment under vacuum or various gas atmospheres (nitrogen and oxygen). Moreover, the emission properties of ZnO can be precisely controlled by introducing certain impurities, by creating phase transformations in sandwich-structured films, and by utilizing various deposition techniques [6–9]. In most cases the photoluminescence properties of ZnO can be modified by doping with metals such as Al, Li, Cu, and Mg, or forming a multilayer film with metal-oxide compounds such as MgO, Al_2O_3, TiO_2, and CuO [10–21]. According to calculations by Yan et al. [22], Cu is one of the most suitable doping metals for ZnO because of its high transition energy and natural abundance. In addition, the van der Waals ionic radii of Cu^+ (0.096 nm) and Cu^{2+} (0.072 nm) are very close to the Zn^{2+} (0.074 nm) ionic radius. Consequently, during doping, Cu^+ and Cu^{2+} ions can be substituted or interstitially located within ZnO [23,24]. In our previous work, doping

Optical Materials EXPRESS

of Cu into ZnO was achieved using sequential deposition of ZnO and Cu thin films by DC magnetron sputtering followed by high temperature annealing in an oxygen environment [25]. The Cu-doped ZnO films obtained demonstrated a blueshifted near-band-edge (NBE) emission peak at 412 nm. However, the peak was still located in the violet region and it may have originated in internal defects in the ZnO film itself, which would imply that the doping process was not responsible. It was assumed that the DC-sputtered ZnO film was too dense for homogenous diffusion from the overlying Cu film. Detailed XPS analysis in previous reports suggests that Cu^{2+} in a free state appears only after heat treatment above 500 °C, which is a more convenient method of replacing Zn atoms. Therefore, direct deposition of CuO instead of metallic Cu film is advantageous for preparation of Cu-doped ZnO thin films.

In this work we report a detailed investigation of structural and optical properties of multilayer ZnO and CuO films deposited by pulsed laser deposition (PLD). The PLD technique was chosen because it allows easy control of the process parameters and is a very convenient method for deposition of multilayer films. It is found that the luminescence properties of the composite films strongly depend on the number of ZnO/CuO layers and demonstrate a stable, temperature-independent redshift of the near-band-edge emission compared to a single layer ZnO thin film. We believe that the proposed ZnO/CuO multilayer architecture offers new insights for fabrication of optical devices such as UV-detectors or blue LEDs, enabling fine control of their optical properties.

2. Experimental

Films of ZnO and CuO were sequentially deposited by pulsed laser deposition to form multilayer structures on thermally-oxidized SiO_2/Si substrates. Amorphous SiO_2/Si substrate was chosen in order to eliminate any substrate effect on the grown film. One-inch cylindrical pellets of ZnO and CuO were prepared by spark plasma sintering at 750 °C [26] using high purity ZnO (99.99%, Sigma Aldrich) and CuO (99.999%, Sigma-Aldrich) nanopowders. An excimer laser (KrF: 248 nm wavelength, 400 µJ pulse power, 5 Hz repetition rate) was used through the experiments. The deposition rates for ZnO and CuO thin films were 0.05 and 0.17 nm/s, respectively, determined by alpha-step thickness measurements. Prior to deposition, all substrates were cleaned ultrasonically with acetone, ethanol, and deionized water for 15 min each. The substrates were transferred into the main chamber (at $5x10^{-7}$ Torr) through a load-lock chamber. Oxygen pressure and substrate temperature in the main chamber were kept at 50 mTorr and 500 °C throughout all deposition processes. Multilayer films were prepared by sequentially depositing 15 nm ZnO and 5 nm CuO films to the desired number of ZnO/CuO layers. Three types of multilayer ZnO/CuO stacks were prepared for investigation, having five, nine, or seventeen layers in total. The five-layered sample, for example, was composed of three ZnO and two CuO layers (ZnO/CuO/ZnO/CuO/ZnO), and was designated ZCZ5. The other samples were designated accordingly as ZCZ9 and ZCZ17. Reference samples of pure ZnO and CuO thin films with 15 nm thickness were also prepared for comparisons. The thickness of the reference samples was chosen based on the fact that it is common for all three types of prepared samples. All samples were annealed at 500 °C for 30 min in an oxygen atmosphere to improve their crystallinity. Crystallography and cross-sectional morphology of prepared films were investigated by powder X-ray diffraction (XRD; Philips X'Pert APD) and scanning transmission electron microscopy (STEM; JSM-6701F). Samples for TEM analysis were prepared by FIB system (Hitachi NB 5000, Japan) in order to provide a better surface for high precision elemental analysis. Reflectance and photoluminescence properties were examined by UV-Vis-NIR spectroscopy (Lambda-750), and a fluorescence spectrometer (JASCO FP-6500) with a 300 nm excitation wavelength, respectively.

Optical Materials EXPRESS

3. Result and discussion

3.1 Cross-sectional microstructure and structural analysis

The cross-sectional morphology and elemental composition of the multilayered films were analyzed by TEM and energy-dispersive X-ray spectroscopy (EDS) techniques and the results are presented in Fig. 1. Figures 1(a)–1(c) shows cross-section bright-field TEM and EDS elemental mapping images for the ZCZ5, ZCZ9, and ZCZ17 samples. The bright-field TEM images clearly show multilayered films composed of alternately-deposited ZnO and CuO layers, with total thicknesses of 55, 95, and 295 nm for the ZCZ5, ZCZ9, and ZCZ17 samples, respectively. The distributions of Zn, O, and Cu within the multilayered films are presented in the EDS mapping images (see Figs. 1(a′), 1(b′), and 1(c′), respectively).

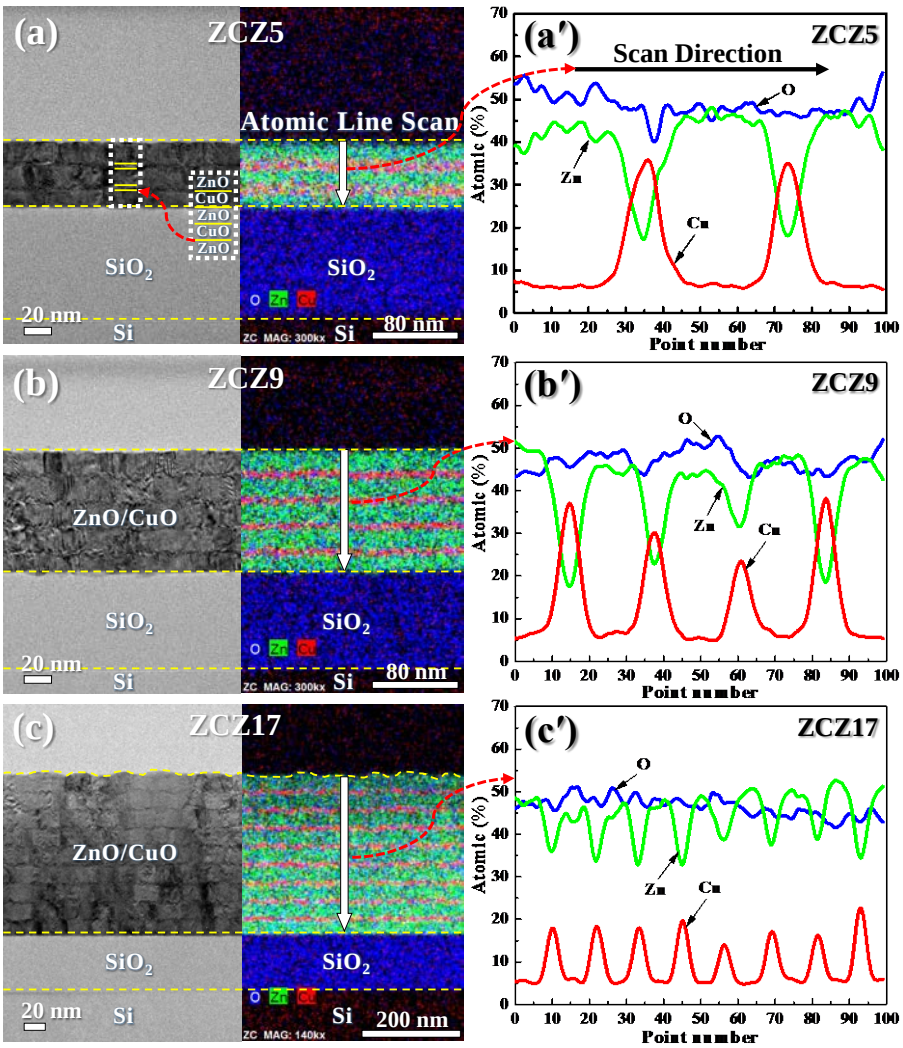

Fig. 1. Cross-sectional TEM analysis of the alternating ZnO/CuO multilayered films. (a)–(c) bright-field TEM and EDS elemental mapping of (a) ZCZ5, (b) ZCZ9, and (c) ZCZ17 films. (a′)–(c′) shows atomic scan line profiles acquired from the corresponding films.

Optical Materials EXPRESS

Table 1. Average atomic percentages of Zn, Cu and O elements in ZnO/CuO multilayer thin films from TEM-EDS analysis.

Sample ID	Element compositions (at.%)			Total thickness (nm)
	Zn	Cu	O	
ZCZ5	39.65	11.75	48.6	55
ZCZ9	40.26	12.69	47.05	95
ZCZ17	44.41	9.1	46.49	295

Line profiles across the thin films in Figs. 1(a′), 1(b′), and 1(c′) show the distributions of Zn, Cu, and O atoms. Atomic percentage allocations of elements are summarized in Table 1. The values given in Table 1 suggest that the average atomic percentages of Zn and Cu increase slightly with increasing ZnO/CuO stack numbers (ZCZ5 to ZCZ9). With the ZCZ17 film, the atomic percentage of Zn increases further, while that of Cu decreases. This change is attributed to the substitutional and interstitial behavior of Cu atoms in the ZnO structure. The variation of O atom percentage is attributed to the formation of oxygen vacancies and possible relocation of Zn and Cu atoms from oxygen sites. In addition, line profiles reveal the presence of Zn and Cu in the CuO and ZnO regions, respectively, indicating interfusion of layers. As can be seen, the percentages of Zn atoms in the CuO regions are 16.5, 17.2, and 35 at.% for increasing stack numbers of ZnO/CuO layers. Crystallographic behavior of the multilayered films was further analyzed by XRD and is presented in Fig. 2. Figure 2(a) shows two distinct ZnO reflection peaks of (002) and (103) at 34.1 and 63.1°, respectively, which are assigned to the hexagonal wurtzite structure (PDF#89-1397).

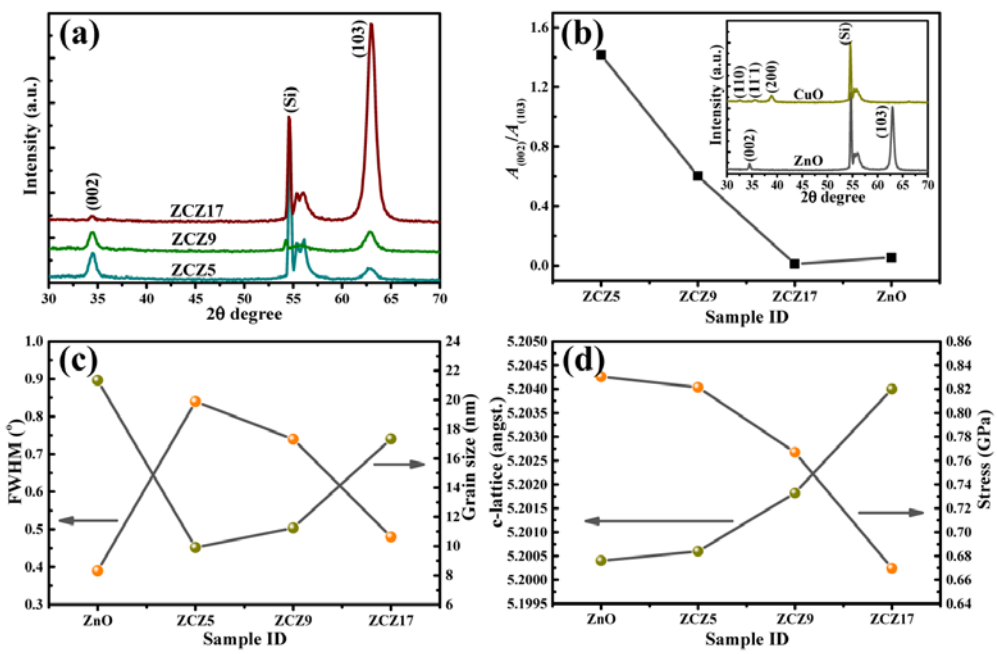

Fig. 2. Microstructural analysis of ZnO/CuO multilayer films deposited by pulsed laser deposition techniques. (a) X-ray diffraction patterns of ZnO/CuO multilayer films on SiO_2/Si substrate. (b) Graph showing dependence of areal ratio of (002) and (103) planes on ZnO/CuO stack number, and (inset) the single layer ZnO thin film used as a reference sample. (c) Relationship between FWHM and grain size calculated for ZnO (002) plane. (d) Dependence of lattice parameter c and residual stress on the ZnO/CuO stack number.

Optical Materials EXPRESS

Table 2. Parameters of the (002) diffraction peak of bare ZnO and ZnO/CuO multilayer films.

Sample ID	Peak center (2 theta)	FWHM, (degree)	d-spacement, (Angst.)	c-lattice, (Angst.)	Grain size, (nm)	Residual stress, (GPa)	L-bonding length, (Angst.)
ZnO	34.464	0.39	2.6002	5.2004	21.32	0.8303	1.9834
ZCZ5	34.463	0.89	2.6003	5.2006	9.902	0.8214	1.9846
ZCZ9	34.455	0.74	2.6009	5.2018	11.24	0.7669	1.9848
ZCZ17	34.440	0.48	2.6020	5.2040	17.32	0.6696	1.9731

An intense, sharp peak observed at 54.5° in all samples is assigned to reflection from the Si (004) plane of the much thicker Si substrates. All three multilayered films (ZCZ5, ZCZ9, and ZCZ17) exhibit only ZnO reflection peaks, without additional Cu/CuO peaks. An apparent absence of the Cu/CuO reflection in the multilayer samples could be the result of lower CuO content within the stacked films (thicknesses of ZnO and CuO layers are 15 and 5 nm, respectively). Nevertheless, it can be seen that the intensities of the ZnO (002) and (103) peaks are greatly influenced by the number of ZnO/CuO layers, which can be explained by impurity dopant and intrinsic defect effects [27]. In Fig. 2(a) the feature at 34.1° for the (002) plane is the dominant peak for the ZCZ5 sample. By increasing the number of ZnO/CuO layers (ZCZ5→ZCZ9→ZCZ17), the intensity of the (002) reflection peak decreases, while the (103) peak is raised. This indicates that the dominant ZnO plane changes from (002) to (103) as the amount of Cu-dopant impurity increases, at the same time suggesting an increase of intrinsic defects in the ZnO structure. The variation of the ratio of areas under the (002) and (103) peaks (A(002)/A(103)) with ZnO/CuO stack layer number is plotted in Fig. 2(b). Inset of the Fig. 2(b) shows XRD characteristics of a single layer ZnO and CuO thin films for comparison. To further understand the effect of Cu-doping, the full width at half maximum (FWHM) of the ZnO (002) diffraction peak was analyzed to give grain size, lattice parameter c, and residual stress (see Figs. 2(c) and 2(d)). Figure 2(c) shows the grain size calculated from the FWHM as a function of the number of ZnO/CuO layers. It can be seen that ZnO grain size of the film is dramatically decreased by introducing two layers of CuO film in sample ZCZ5. By further increasing the number of CuO layers (samples ZCZ9 and ZCZ17) the grain size slightly increases. Figure 2(d) indicates that the ZnO film has the smallest lattice parameter of 5.2004 Å and the highest residual stress of 0.83 GPa, while the residual stress in ZCZ multilayer films linearly decreases with increasing number of CuO layers. The increase observed in the lattice parameter could result from the contribution of Cu atoms that originate in the CuO films. The detailed values of the parameters calculated from the data are given in Table 2.

Figure 3 shows HR-TEM images of the ZnO/CuO/ZnO interface. From Figs. 3(a) and 3(b) we can see that both the ZnO and CuO films are highly crystalline and the transition through their interface is gradual. We can also observe minor, ≤ 0.5 nm, thickness variation in CuO layer. We believe that this small thickness fluctuation will not have significant effect on the interfacial crystallographic properties of the films. The inset in Fig. 3(a) shows enlarged HR-TEM images of the CuO and ZnO regions. The lattice fringes of 0.235 nm for the CuO and 0.261 nm for the ZnO planes are well matched with the CuO (111) and ZnO (002) planes. However, close analysis of the ZnO/CuO interface lattice reveals that the ZnO layers contain numerous crystallographic defects, such as crystal dislocations, and interstitial and vacancy defects, as a result of introduction of the CuO layers between them. These defects can be clearly observed in the insets of Fig. 3(b). Arrowheads in inset-1 and inset-2 show Zn-to-Zn interstitial and Cu substitutional defects, respectively. We assume that during the heat treatment Cu atoms from the CuO layer uniformly diffuse into the ZnO layer and substitute

Optical Materials EXPRESS

for Zn atoms, forming Cu substitutional defects. Displaced Zn atoms locate at interstitial sites of the ZnO structure, forming Zn-to-Zn defects. The effects of these defects on the optical properties of the films are discussed in detail in Section 3.2.

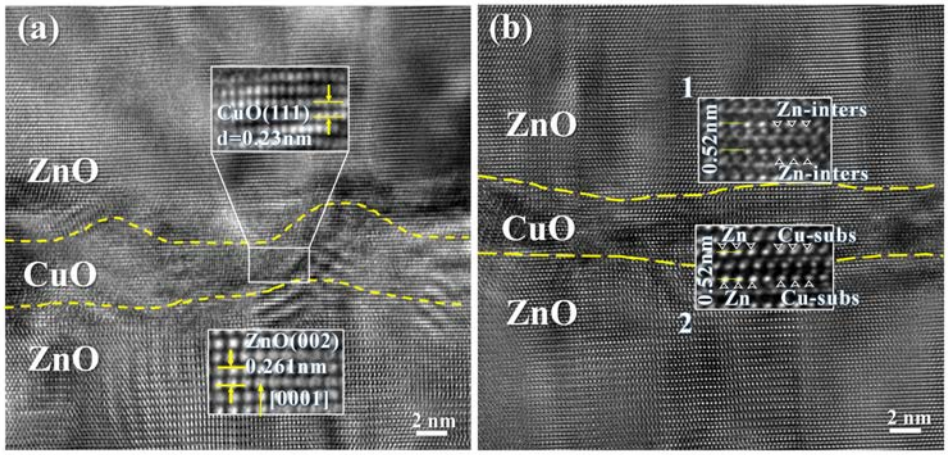

Fig. 3. HR-TEM images of the ZCZ17 sample at the ZnO/CuO interface. Insets in (a) show HR-TEM images of ZnO and CuO regions of the multilayer film. Insets in (b) clearly show Zn-to-Zn interstitial and Cu substitutional defects.

3.2 Optical analysis

Photoluminescence (PL) properties of the ZnO and ZnO/CuO-multilayer films are shown in Fig. 4. From the normalized photoluminescence (NPL) curves in Fig. 4(a) it is clearly seen that, with the introduction of the CuO and the increase in layer numbers, the near-band-edge emission (NBE) peak is continuously redshifted from 385 nm to 425 nm, and the intensity of the deep level emission (DLE) peak centered at 564 nm increases. The behavior of the blue emission in the band centered at 465 nm, however, is not strictly in proportion with the CuO layer number throughout the range, i.e. the intensity of the emission peak initially increases from ZCZ5 to ZCZ9, but then slightly decreases for ZCZ17. Further, the PL spectra from Fig. 4(a) were fitted by Gaussian functions as shown in Figs. 4(b)–4(e). Figure 4(f) shows a schematic of the emission band diagram of CuO/ZnO film [1,6,28]. The fitted spectrum of the single ZnO thin film reveals four peaks, shown in Fig. 4(b). The peaks numbered 1 (385 nm) and 4 (544 nm) correspond to the NBE and DLE emission bands of pristine ZnO, which arise from the direct band exciton energy of ZnO and oxygen vacancy (V_O) defects, respectively. Also, the two shoulder peaks numbered 2 (418 nm) and 3 (465 nm) are assigned to Zn-to-Zn interstitials (I_{Zn}) and Zn-vacancy (V_{Zn}) defects, respectively. Photoluminescence spectra of the multilayered samples indicate that the NBE peak (number 1, 400 nm) is redshifted, while the DLE peak (number 4, 514 nm) is blueshifted. In addition, a new peak at 564 nm (peak number 5) is observed for all multilayer samples and attributed to oxygen interstitials (I_O). On the other hand, Oommen et al. report that the PL peak centered at 564 nm for a CuO/ZnO film is associated with band-to-band emission in Cu_2O or CuO [29].

Optical Materials EXPRESS

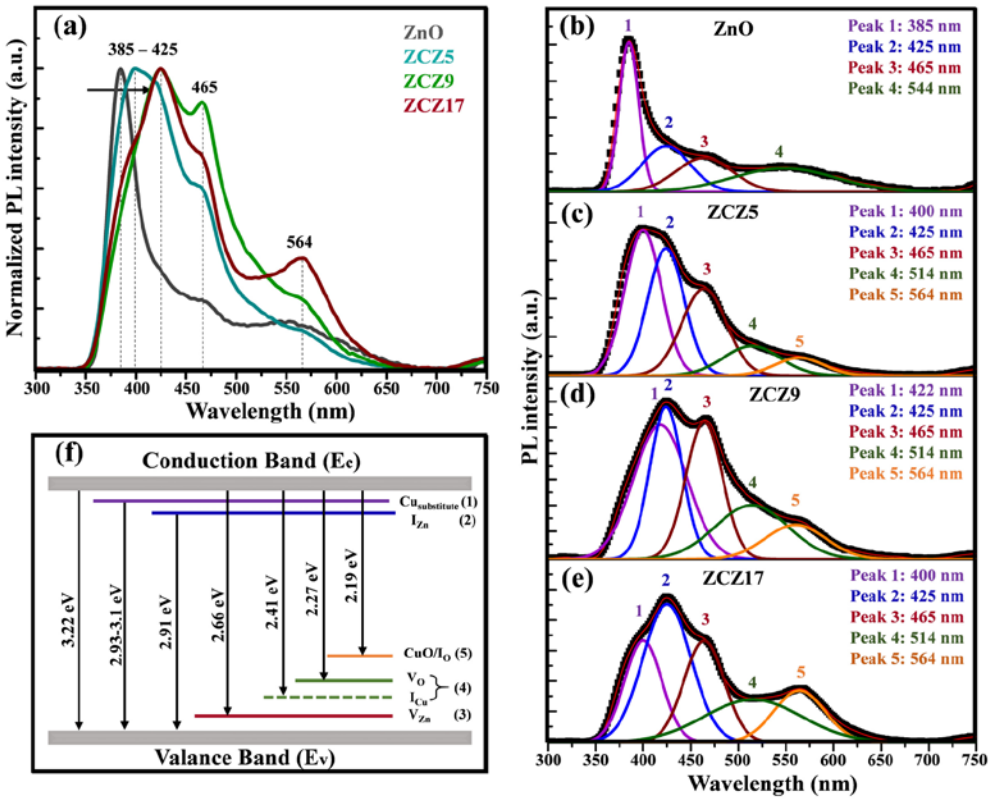

Fig. 4. Photoluminescence properties of ZnO/CuO multilayer films. (a) Normalized photoluminescence spectra of pristine-ZnO and ZnO/CuO multilayer films. (b)–(e) Gaussian fitted curves for ZnO, ZCZ5, ZCZ9, and ZCZ17 films. (f) Schematic of Cu-doped ZnO band diagram.

Indeed, the intensity of the 564 nm peak (number 5) increases linearly with the number of CuO layers. Overall, close examination of the fitted PL curves suggests that the NBE emission peak of the ZnO film is redshifted by introducing and increasing the CuO layer number up to nine as follows; ZnO@385 nm → ZCZ5@400nm → ZCZ9@422 nm. However, further increase of the CuO content (sample ZCZ17) leads to a backward shift of the NBE peak (to 400 nm), and an increase of the CuO-related emission peak (peak number 5@564 nm). The optical properties of the samples were further analyzed by UV-VIS-NIR reflectance spectroscopy as presented in Fig. 5(a). It can be seen that the main absorption peak of the pure ZnO film at short wavelengths (below 400 nm) is redshifted by introducing CuO layers (sample ZCZ5). In the case of the ZCZ9 sample, the UV absorption edge is further redshifted and an additional absorption peak centered at 555 nm appears. The results indicate that the bandgap of pure ZnO is modified by introducing Cu atoms into the ZnO lattice. The optical bandgap of the samples were determined by a Tau′c plot, based on the expression:

$$(h\nu\alpha)^{1/2} = A(h\nu - E_g) \tag{1}$$

Where h is Planck's constant, ν is the light frequency, α is the absorption coefficient, E_g is the bandgap, and A is a proportionality constant. The optical bandgap E_g is estimated by

Optical Materials EXPRESS

plotting $(h\nu\alpha)^2$ versus the photon energy $h\nu$ and extrapolating the linear region of the curve to the energy axis.

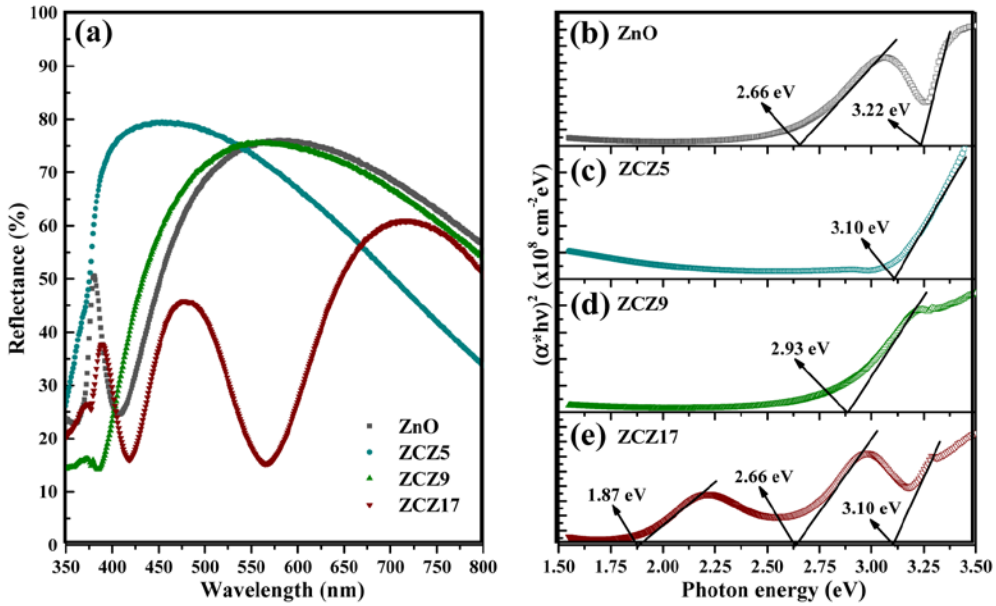

Fig. 5. Reflectance spectra and Tau′c plots of the ZnO and ZnO/CuO multilayer films.

The Tau′c plot of the ZnO film in Fig. 5(b) shows two bandgap values of 3.22 eV and 2.66 eV, corresponding to the NBE and DLE bands, respectively. For the ZnO/CuO multilayer samples, the NBE bandgap values for ZCZ5 and ZCZ9 are slightly decreased to 3.10 and 2.93 eV, respectively (see Figs. 5(c) and 5(d)). By further increasing the number of CuO layers, both the near-band-edge and the deep level emission bands decrease in energy. In the ZCZ17 sample, an additional band edge at 1.87 eV is observed and is assigned to the CuO band edge (Fig. 5(e)).

4. Conclusion

In conclusion, the near-band-edge emission peak of ZnO is redshifted from 385 nm to 422 nm by effective Cu-doping during formation of ZnO/CuO multilayer films. This redshift is linear in the number of ZnO/CuO stacked layers, up to nine. This shift is mainly attributed to the formation and increase of Cu substitutional and Zn-to-Zn interstitial defects, as confirmed by HR-TEM analysis. A subsequent shift of the NBE peak back to 400 nm is observed when the number of ZnO/CuO layers is increased to seventeen, and is associated with an increase of Zn-to-Zn interstitial defects in the multilayered film. The key findings of this study suggest that the photoluminescence properties of ZnO film can be controlled by introducing a specified number of CuO thin films alternating with ZnO layers.

Funding

Basic research program through the Daegu Gyeongbuk Institute of Science and Technology (DGIST), funded by the Ministry of Science, ICT and Future Planning of Korea (16-NB-05).